Electronic Supplementary Material (ESI) for CrystEngComm.

Electronic Supplementary Information

Crystal structures at ambient pressure

Table 1: Refined atomic positions, occupancy factors (F), and displacement parameters (Uiso) for dehydrated K-L determined from ToF neutron diffraction data collected on the POLARIS instrument at ambient pressure

Atom Type	Label	x	y	z	F	Uiso	Wyckoff Site Symmetry
K	K_1	0.3333	0.6667	0.5	1	0.026(2)	2d *-6m2(100)*
K	K_2	0	0.5	0.5	1	0.026(2)	3g *mmm(010)*
K	K_3	0	0.3178(8)	0	0.57	0.026(2)	6j *mm2(010)*
O	O_1	0	0.27365(24)	0.5	1	0.0107(2)	6k *mm2(010)*
O	O_2	0.1640(5)	0.3277	0.5	1	0.0107(2)	6m *mm2(101)*
O	O_3	0.2651(3)	0.5275	0.2537(4)	1	0.01334	12o *m(100)*
O	O_4	0.10173(12)	0.41455(14)	0.32241(22)	1	0.0107(2)	24r *1*
O	O_5	0.4267(4)	0.8526	0.2738(3)	1	0.0107(2)	12p *m(100)*
O	O_6	0.14501(17)	0.47680(16)	0	1	0.0107(2)	12p *m(001)*
Si	Si_1	0.09310(24)	0.35739(27)	0.5	0.767	0.009(1)	12q *m(001)*
Al	Al_1	0.09310(24)	0.35739(27)	0.5	0.233	0.009(1)	12q *m(001)*
Si	Si_2	0.16507(22)	0.49751(20)	0.21207(30)	0.767	0.0081(6)	24r *1*
Al	Al_2	0.16507(22)	0.49751(20)	0.21207(30)	0.233	0.0081(6)	24r 1

Table 2: Rietveld refinement parameters for dehydrated K-L determined from ToF neutron diffraction data collected on the POLARIS instrument at ambient pressure

data range (*d*-spacing) (Å)	0.6-13
no. of observations	9518
no. of variables	67
a (Å)	18.4199(6)
c (Å)	7.4937(2)
volume (Å^3)	2201.92(9)
R_{exp}	1.21
R_{wp}	2.00
reduced $\chi^2 = (R_{wp}/R_{exp})^2$	2.72
GOF $= (R_{wp}/R_{exp})^2$	1.65

Table 3: Refined atomic positions, occupancy factors (F), and displacement parameters (Uiso) for dehydrated K-L with m.e., determined from ToF neutron diffraction data collected on the PEARL instrument at ambient pressure

Atom Type	Label	x	y	z	F	Uiso	Wyckoff Site Symmetry
K_1	K	0.3333	0.6667	0.5	1	0.030(5)	2d *-6m2(100)*
K_2	K	0	0.5	0.5	1	0.03	3g *mmm(010)*
K_3	K	0	0.2994(21)	0	0.57	0.03	6j *mm2(010)*
O_1	O	0	0.2698(8)	0.5	1	0.0203(9)	6k *mm2(010)*
O_2	O	0.1647(13)	0.3295	0.5	1	0.0203	6m *mm2(101)*
O_3	O	0.2637(11)	0.5274	0.2494(13)	1	0.0203	12o *m(100)*
O_4	O	0.1039(4)	0.4137(5)	0.3197(7)	1	0.0203	24r 1
O_5	O	0.4265(14)	0.853	0.2753(11)	1	0.0203	12p *m(100)*
O_6	O	0.1413(6)	0.4770(6)	0	1	0.0203	12p *m(001)*
Si_1	Si	0.0921	0.3578	0.5	1	0.014	12q *m(001)*
Si_2	Si	0.1665	0.5019	0.2102	0.767	0.0193	24r 1
Al_1	Al	0.0921(8)	0.3578(8)	0.5	0.767	0.014(3)	12q *m(001)*
Al_2	Al	0.1665(7)	0.5019(7)	0.2102(10)	0.233	0.0193(21)	24r 1
w7	O	0.132(3)	0.0658	0.282(7)	0.268(20)	0.065	12o *m(010)*
w6	O	0.268(3)	0.1338	0	0.332(31)	0.065	6l *mm2(210)*
w5	O	0	0.1570(31)	0.356(6)	0.233(21)	0.065	12n *m(210)*
w4	O	0	0	0.081(9)	0.36(5)	0.065	2e *6mm(100)*
w3	O	0.1184(31)	0.237	0.159(4)	0.485(25)	0.065	12o *m(100)*

Table 4: Refinement parameters for dehydrated K-L with m.e., determined from ToF neutron diffraction data collected on the PEARL instrument at ambient pressure

data range (*d*-spacing) (Å)	0.7-4
no. of observations	2948
no. of variables	51
a (Å)	18.3786(15)
c (Å)	7.5277(4)
volume (Å^3)	2202.02(21)
R_{exp}	1.66
R_{wp}	1.43
reduced $\chi^2 = (R_{wp}/R_{exp})^2$	0.74
GOF $= (R_{wp}/R_{exp})^2$	0.86

Compression data

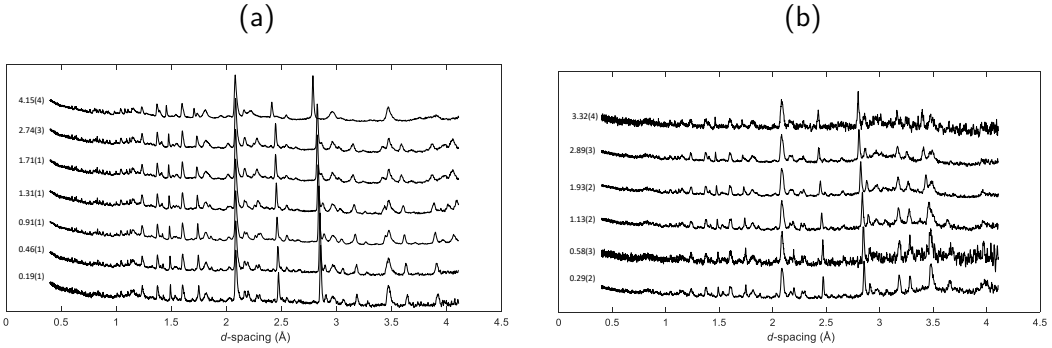

Figure 1: Experimental ToF neutron diffraction patterns with increasing pressure for K-L using (a) Fluorinert as a non-penetrating PTM and (b) a 4:1 mixture of perdeuterated methanol:ethanol (m.e.) as a penetrating PTM. Pressure is given in GPa

Crystal structures at high-pressures

Non-penetrating media

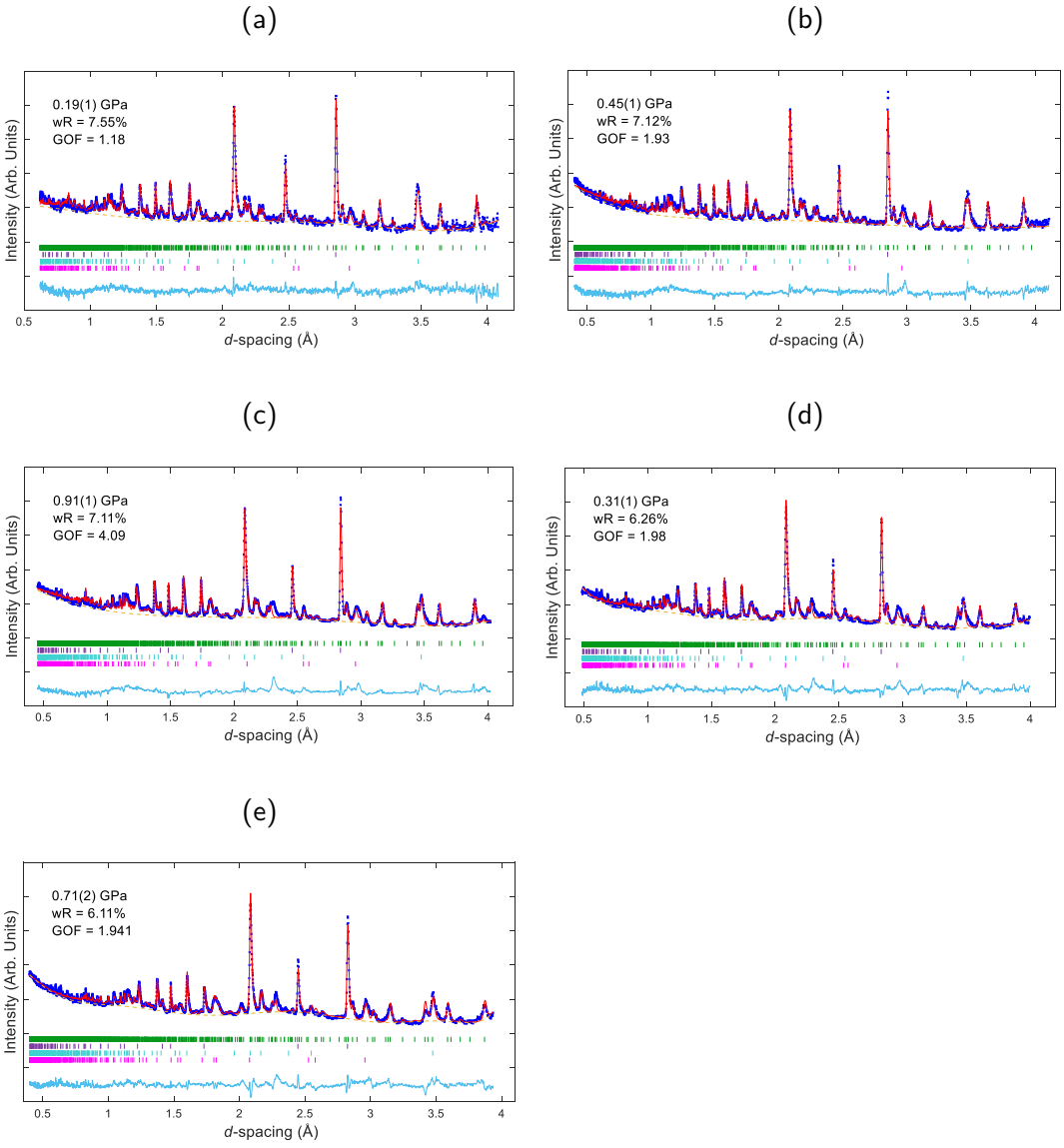

Figure 2: TOF, neutron powder diffraction data with associated Rietveld refinement fits for K-L (a-e) from 0.19(1) to 1.71(2) GPa. Observed and calculated profiles are shown as blue crosses and red lines, respectively. Backgrounds are plotted with orange dotted lines. The residual (observed minus calculated intensity) plot is shown below as a cyan line. Bragg reflections for each phase are marked with vertical bars; K-L in green, Pb in purple, Alumina in cyan and Zirconia in pink.

Table 5: Refined atomic positions, occupancy factors (F), and displacement parameters (Uiso) for K-L at the investigated pressure points where Rietveld refinement was possible. Structures are determined from ToF neutron diffraction data collected on the PEARL instrument, using Fluorinert as a non-penetrating PTM. GASP-simulated structures were used as input models for refinement

Atom Type	Label	x	y	z	F	Uiso	Wyckoff Site Symmetry
			0.19(1) GPa				
K_1	K	0.33333	0.66667	0.5	1	0.02	2d *-6m2(100)*
K_2	K	0	0.5	0.5	1	0.02	3g *mmm(010)*
K_1	K	0.33333	0.66667	0.5	1	0.02	2d *-6m2(100)*
K_2	K	0	0.5	0.5	1	0.02	3g *mmm(010)*
K_3	K	0	0.3178	0	0.57	0.02	6j *mm2(010)*
O_1	O	1	0.2740(13)	0.5	1	0.008	6k *mm2(010)*
O_2	O	0.1618(10)	0.3236	0.5	1	0.008	6m *mm2(101)*
O_3	O	0.2660(10)	0.532	0.2432(25)	1	0.008	12o *m(100)*
O_4	O	0.1064(8)	0.4139(8)	0.3254(11)	1	0.008	24r *1*
O_5	O	0.4256(10)	0.8512	0.2755(24)	1	0.008	12p *m(100)*
O_6	O	0.1457(12)	0.4798(11)	1	1	0.008	12p *m(001)*
Si_1	Si	0.0941(7)	0.3560(8)	0.5	1	0.008	12q *m(001)*
Si_2	Si	0.1672(8)	0.4995(7)	0.2106(11)	1	0.008	24r 1
			0.45(1) GPa				
K_1	K	0.33333	0.66667	0.5	1	0.02	2d *-6m2(100)*
K_2	K	0	0.5	0.5	1	0.02	3g *mmm(010)*
K_3	K	0	0.3178	0	0.57	0.02	6j *mm2(010)*
O_1	O	1	0.2767(16)	0.5	1	0.008	6k *mm2(010)*
O_2	O	0.1584(14)	0.3169	0.5	1	0.008	6m *mm2(101)*
O_3	O	0.2665(14)	0.5331	0.2395(28)	1	0.008	12o *m(100)*
O_4	O	0.1053(10)	0.4138(9)	0.3249(15)	1	0.008	24r 1
O_5	O	0.4230(14)	0.846	0.2804(26)	1	0.008	12p *m(100)*
O_6	O	0.1474(14)	0.4798(13)	1	1	0.008	12p *m(001)*
Si_1	Si	0.0942(10)	0.3568(11)	0.5	1	0.008	12q *m(001)*
Si_2	Si	0.1684(10)	0.4998(10)	0.2093(16)	1	0.008	24r 1

0.91(1) GPa							
K_1	K	0.33333	0.66667	0.5	1	0.02	2d *-6m2(100)*
K_2	K	0	0.5	0.5	1	0.02	3g *mmm(010)*
K_3	K	0	0.3178	0	0.57	0.02	6j *mm2(010)*
O_1	O	1	0.2743(21)	0.5	1	0.008	6k *mm2(010)*
O_2	O	0.1590(24)	0.318	0.5	1	0.008	6m *mm2(101)*
O_3	O	0.2636(22)	0.527	0.243(4)	1	0.008	12o *m(100)*
O_4	O	0.1035(12)	0.4119(11)	0.3236(21)	1	0.008	24r 1
O_5	O	0.4223(21)	0.845	0.283(3)	1	0.008	12p *m(100)*
O_6	O	0.1429(16)	0.4723(15)	1	1	0.008	12p *m(001)*
Si_1	Si	0.0958(17)	0.3578(16)	0.5	1	0.008	12q *m(001)*
Si_2	Si	0.1675(16)	0.4968(14)	0.2148(25)	1	0.008	24r 1
1.31(1) GPa							
K_1	K	0.33333	0.66667	0.5	1	0.02	2d *-6m2(100)*
K_2	K	0	0.5	0.5	1	0.02	3g *mmm(010)*
K_3	K	0	0.313	0	0.57	0.02	6j *mm2(010)*
O_1	O	1	0.2733(15)	0.5	1	0.008	6k *mm2(010)*
O_2	O	0.1584(14)	0.3168	0.5	1	0.008	6m *mm2(101)*
O_3	O	0.2625(14)	0.525	0.2526(30)	1	0.008	12o *m(100)*
O_4	O	0.1045(9)	0.4125(8)	0.3251(14)	1	0.008	24r 1
O_5	O	0.4218(13)	0.8435	0.2685(26)	1	0.008	12p *m(100)*
O_6	O	0.1425(12)	0.4687(11)	1	1	0.008	12p *m(001)*
Si_1	Si	0.0938(10)	0.3556(10)	0.5	1	0.008	12q *m(001)*
Si_2	Si	0.1649(11)	0.4956(9)	0.2133(16)	1	0.008	24r 1
1.71(2) GPa							
K_1	K	0.33333	0.66667	0.5	1	0.02	2d *-6m2(100)*
K_2	K	0	0.5	0.5	1	0.02	3g *mmm(010)*
K_3	K	0	0.3178	0	0.57	0.02	6j *mm2(010)*
O_1	O	1	0.2761(16)	0.5	1	0.008	6k *mm2(010)*
O_2	O	0.1559(14)	0.3118	0.5	1	0.008	6m *mm2(101)*
O_3	O	0.2622(14)	0.5243	0.256(3)	1	0.008	12o *m(100)*
O_4	O	0.1070(10)	0.4135(9)	0.3256(16)	1	0.008	24r 1
O_5	O	0.4255(13)	0.851	0.2657(30)	1	0.008	12p *m(100)*
O_6	O	0.1387(13)	0.4633(13)	1	1	0.008	12p *m(001)*
Si_1	Si	0.0926(9)	0.3530(11)	0.5	1	0.008	12q *m(001)*
Si_2	Si	0.1643(11)	0.4966(9)	0.2124(17)	1	0.008	24r 1

Table 6: Refinement parameters for K-L at the investigated pressure points, determined from ToF neutron diffraction data collected on the PEARL instrument using Fluorinert as a non-penetrating PTM

Pressure (GPa)	0.19(1)	0.45(1)	0.91(1)	1.31(1)	1.71(2)
data range (*d*-spacing) (Å)	0.6-4	0.6-4	0.4-4	0.48-4	0.4-4
no. of observations	3140	3881	3634	3512	3809
no. of variables	32	32	32	36	36
a (Å)	18.391(5)	18.351(5)	18.292(6)	18.249(4)	18.186(5)
c (Å)	7.4791(12)	7.4567(12)	7.4300(14)	7.4015(11)	7.3673(12)
volume (Å^3)	2190.9(7)	2174.7(7)	2153.0(8)	2134.8(6)	2110.3(7)
R_{exp}	6.40	3.69	1.74	3.16	3.20
R_{wp}	7.55	7.12	7.11	6.26	6.11
reduced $\chi^2 = (R_{wp}/R_{exp})^2$	1.39	3.72	16.73	3.92	3.65
GOF $= (R_{wp}/R_{exp})$	1.18	1.93	4.09	1.98	1.91

Table 7: Interatomic distances (Å) for K-L at the investigated pressure points

Pressure (GPa)	P_{amb}	0.19(1)	0.45(1)	0.91(1)	1.31(1)	1.71(2)
T1-O1	1.635(2)	1.631(10)	1.613(15)	1.651(26)	1.616(15)	1.562(13)
T1-O2	1.645(9)	1.626(12)	1.676(18)	1.65(4)	1.658(19)	1.657(17)
T1-O4	1.655(2)	1.628(7)	1.618(11)	1.605(19)	1.607(11)	1.626(11)
T2-O3	1.657(6)	1.623(11)	1.600(18)	1.57(3)	1.608(18)	1.621(17)
T2-O4	1.612(2)	1.645(10)	1.659(15)	1.616(26)	1.586(15)	1.579(15)
T2-O5	1.659(7)	1.647(11)	1.653(18)	1.68(3)	1.642(18)	1.622(18)
T2-O6	1.633(2)	1.620(9)	1.601(12)	1.653(18)	1.641(11)	1.659(12)
Average	1.642	1.631	1.634	1.632	1.623	1.618
K1-O3	2.855(2)	2.879(12)	2.881(14)	2.932(17)	2.894(13)	2.873(15)
K2-O5	2.889(2)	2.905(10)	2.951(11)	2.937(12)	3.016(11)	2.913(13)
K3-O4	3.031(4)	3.069(11)	3.051(13)	3.017(15)	3.047(11)	3.013(1)
K3-O6	2.809(9)	2.842(16)	2.853(18)	2.732(21)	2.734(16)	2.586(19)

Table 8: Bond angles (°) for K-L at the investigated pressure points

Pressure (GPa)	P_{amb}	0.19(1)	0.45(1)	0.91(1)	1.31(1)	1.71(2)
T1- O1 - T1	130.48(28)	133.6(14)	136.0(19)	133.8(27)	133.2(18)	138.2(18)
T1- O2 - T1	146.841(1)	143.1(8)	134.9(11)	134.8(18)	135.7(11)	133.9(11)
T2 - O3 - T2	137.01(10)	138.7(11)	138.0(13)	141.8(17)	140.2(12)	140.9(14)
T2 - O4 - T1	144.07(12)	148.3(8)	146.7(11)	143.6(16)	147.0(10)	150.6(11)
T2 - O5 - T2	141.45(14)	139.7(11)	139.6(14)	141.9(18)	150.1(14)	147.0(15)
T2 - O6 - T2	153.40(16)	152.9(12)	153.3(15)	148.9(21)	148.1(14)	141.3(15)
Average	142.2	142.7	141.4	140.8	142.4	142.0

Table 9: 12-ring channel distances and ellipticity (Å) for K-L at the investigated pressure points

Pressure (GPa)	P_{amb}	0.19(1)	0.45(1)	0.91(1)	1.31(1)	1.71(2)
O1-O1 [001]	10.081(6)	10.07(3)	10.15(4)	10.03(5)	9.97(4)	10.02(4)
O2-O2 [001]	10.465	10.77(2)	10.073(1)	10.075(5)	10.013	9.847
O1-O1 [100]	7.4937(2)	7.479(1)	7.457(1)	7.430(1)	7.402(1)	7.369(2)
12 ring ϵ	1.04	1.07	1.01	1.00	1.00	1.02

Table 10: 8-ring channel distances and ellipticity (Å) for K-L at the investigated pressure points

Pressure (GPa)	P_{amb}	0.19(1)	0.45(1)	0.91(1)	1.31(1)	1.71(2)
O1-O1 [001]	8.339(6)	8.73(3)	8.92(2)	8.97(1)	8.27(3)	8.14(4)
O5-O5 [001]	4.68	4.74	4.895	4.911	4.947	4.693
O5-O5 [100]	3.390(3)	4.12(2)	4.18(2)	3.23(3)	3.43(2)	3.45(3)
8 ring ϵ	1.79	1.84	1.82	1.83	1.67	1.73

Table 11: 6-ring channel distances (Å) for K-L at the investigated pressure points

Pressure (GPa)	P_{amb}	0.19(1)	0.45(1)	0.91(1)	1.31(1)	1.71(2)
O3-O5 [001]	5.1563(1)	5.089(1)	4.982(2)	5.046(2)	5.035	5.1450(4)

Penetrating media

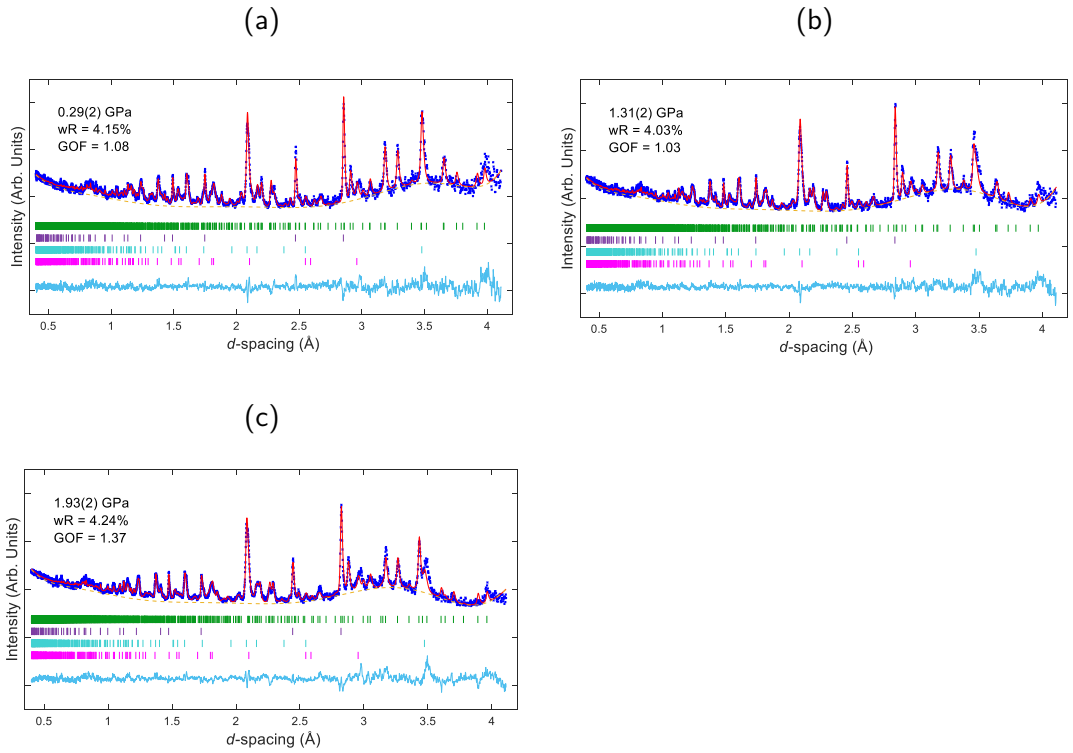

Figure 3: TOF, neutron powder diffraction data with associated Rietveld refinement fits for K-L with m.e. (a-c) from 0.29(2) to 1.93(2) GPa. Observed and calculated profiles are shown as blue crosses and red lines, respectively. Backgrounds are plotted with orange dotted lines. The residual (observed minus calculated intensity) plot is shown below as a cyan line. Bragg reflections for each phase are marked with vertical bars; K-L in green, Pb in purple, Alumina in cyan and Zirconia in pink.

Table 12: Refined atomic positions, occupancy factors (F), and displacement parameters (Uiso) for K-L at the investigated pressure points where Rietveld refinement was possible. Structures are determined from ToF neutron diffraction data collected on the PEARL instrument, using m.e. as a penetrating PTM. GASP-simulated structures were used as input models for refinement

Atom Type	Label	x	y	z	F	Uiso	Wyckoff Site Symmetry
				0.29(2) GPa			
K_1	K	0.33333	0.66667	0.5	1	0.035(12)	2d *-6m2(100)*
K_2	K	0	0.5	0.5	1	0.035	3g *mmm(010)*
K_3	K	0	0.306(5)	0	0.57	0.035	6j *mm2(010)*
O_1	O	1	0.2717(12)	0.5	1	0.0196(13)	6k *mm2(010)*
O_2	O	0.1670(9)	0.334	0.5	1	0.0196	6m *mm2(101)*
O_3	O	0.2637(9)	0.5274	0.2549(22)	1	0.0196	12o *m(100)*
O_4	O	0.1043(6)	0.4162(7)	0.3271(10)	1	0.0196	24r 1
O_5	O	0.4283(10)	0.8567	0.2728(23)	1	0.0196	12p *m(100)*
O_6	O	0.1449(11)	0.4783(11)	0	1	0.0196	12p *m(001)*
Si_1	Si	0.0931(6)	0.3589(8)	0.5	1	0.041(4)	12q *m(001)*
Si_2	Si	0.1655(7)	0.4991(7)	0.2123(11)	1	0.041	24r 1
w7	O	0.026(11)	0.051	0.216(17)	0.23(4)	0.065	12o *m(010)*
w6	O	0.2919(25)	0.146	0	0.89(5)	0.065	6l *mm2(210)*
w5	O	0	0.127(8)	0.253(26)	0.18(4)	0.065	12n *m(210)*
w3	O	0.2309(21)	0.1154	0.180(5)	0.77(5)	0.065	12o *m(100)*
				1.13(2) GPa			
K_1	K	0.33333	0.66667	0.5	1	0.004	2d *-6m2(100)*
K_2	K	0	0.5	0.5	1	0.004	3g *mmm(010)*
K_3	K	0	0.314(5)	0	0.4857(17)	0.004	6j *mm2(010)*
O_1	O	1	0.2695(10)	0.5	1	0.0052(9)	6k *mm2(010)*
O_2	O	0.1715(8)	0.3431	0.5	1	0.0052	6m *mm2(101)*
O_3	O	0.2634(8)	0.5269	0.2623(21)	1	0.0052	12o *m(100)*
O_4	O	0.1006(6)	0.4145(7)	0.3240(9)	1	0.0052	24r 1
O_5	O	0.4291(9)	0.8582	0.2707(21)	1	0.0052	12p *m(100)*
O_6	O	0.1463(10)	0.4768(9)	0	1	0.0052	12p *m(001)*
Si_1	Si	0.0916(6)	0.3590(7)	0.5	1	0.045(5)	12q *m(001)*
Si_2	Si	0.1648(7)	0.4980(7)	0.2138(11)	1	0.045	24r 1
w7	O	0.02441(20)	0.04882	0.218(17)	0.20(3)	0.065	12o *m(010)*
w6	O	0.2883(24)	0.1441	0	1	0.065	6l *mm2(210)*
w5	O	0	0.115(5)	0.264(17)	0.31(5)	0.065	12n *m(210)*
w3	O	0.2276(20)	0.1138	0.178(5)	0.89(6)	0.065	12o *m(100)*
K_4	K	0	0.5	0	0.2	0.004	3f *mmm(010)*

			1.93(2) GPa				
K_1	K	0.33333	0.66667	0.5	1	0.026(6)	2d *-6m2(100)*
K_2	K	0	0.5	0.5	1	0.026	3g *mmm(010)*
K_3	K	0	0.311(8)	0	0.25	0.026	6j *mm2(010)*
O_1	O	1	0.2705(11)	0.5	1	0.0079(9)	6k *mm2(010)*
O_2	O	0.1673(10)	0.3346	0.5	1	0.0079	6m *mm2(101)*
O_3	O	0.2708(10)	0.5418	0.2266(18)	1	0.0079	12o *m(100)*
O_4	O	0.1020(6)	0.4135(6)	0.3234(11)	1	0.0079	24r 1
O_5	O	0.4195(10)	0.8389	0.2892(17)	1	0.0079	12p *m(100)*
O_6	O	0.1455(10)	0.4784(9)	0	1	0.0079	12p *m(001)*
Si_1	Si	0.0910(8)	0.3579(8)	0.5	1	0.046(4)	12q *m(001)*
Si_2	Si	0.1688(8)	0.4989(7)	0.2109(13)	1	0.046	24r 1
w7	O	0.021(19)	0.0405	0.217(24)	0.13(5)	0.065	12o *m(010)*
w6	O	0.2865(26)	0.1432	0	0.68(5)	0.065	6l*mm2(210)*
w5	O	0	0.120(4)	0.289(12)	0.47(5)	0.065	12n *m(210)*
w3	O	0.223(4)	0.1116	0.201(14)	0.33(5)	0.065	12o *m(100)*
K_4	K	0	0.5	0	0.631	0.026	3f *mmm(010)*

Table 13: Refinement parameters for K-L at the investigated pressure points, determined from ToF neutron diffraction data collected on the PEARL instrument using m.e. as a penetrating PTM

Pressure (GPa)	0.29(2)	1.13(2)	1.93(2)
data range (*d*-spacing) (Å)	0.4-4	0.4-4	0.4-4
no. of observations	3881	3881	3881
no. of variables	51	48	51
a (Å)	18.364(4)	18.324(4)	18.291(4)
c (Å)	7.5108(11)	7.4583(12)	7.3987(10)
volume (Å^3)	2193.6(5)	2168.5(6)	2143.6(6)
R_{exp}	3.84	3.91	3.98
R_{wp}	4.15	4.03	4.24
reduced $\chi^2 = (R_{wp}/R_{exp})^2$	1.17	1.06	1.88 6
GOF $= (R_{wp}/R_{exp})$	1.08	1.03	1.37

Table 14: Interatomic distances (Å) for K-L with m.e. at the investigated pressure points.

Pressure (GPa)	P_{amb}	0.29(2)	1.13(2)	1.93(2)
T1-O1	1.656(6)	1.658(9)	1.660(9)	1.632(11)
T1-O2	1.658(24)	1.635(11)	1.630(10)	1.650(13)
T1-O4	1.650(6)	1.619(7)	1.618(6)	1.605(8)
T2-O3	1.631(19)	1.639(11)	1.650(10)	1.627(13)
T2-O4	1.663(7)	1.616(9)	1.613(9)	1.648(11)
T2-O5	1.604(24)	1.641(11)	1.645(10)	1.673(13)
T2-O6	1.6478(24)	1.639(8)	1.636(8)	1.612(10)
Average T-O	1.644	1.635	1.636	1.635
K1-O3	2.911(6)	2.879(11)	2.840(10)	2.830(9)
K2-O5	2.888(5)	2.847(10)	2.826(9)	2.991(7)
K3-O4	3.137(15)	3.147(29)	3.040(28)	3.03(5)
K3-O6	2.988(30)	2.94(6)	2.82(6)	2.88(10)
K4-O5			3.023(10)	3.330(8)
K4-O6			2.918(19)	2.880(19)
K3-w6	2.80(5)	2.82(5)	2.90(6)	2.87(10)
K3-w3	3.16(5)	3.35(7)	3.45(7)	3.50(13)
w3-O2	2.964(25)	2.91(4)	3.02(3)	2.83(9)
w5-O1	2.44(6)	3.24(18)	3.34(9)	3.17(8)
w3-w7	1.91(6)	2.87(4)	2.852(31)	3.3(3)
w3-w6	1.29(3)	1.67(3)	1.64(3)	1.79(9)
w3-w5	2.43(5)	2.09(8)	2.17((8)	2.08(6)
w4-w7	2.58(6)			
w5-w7	3.11(6)	1.70(26)	1.52(9)	1.74(27)
w6-w7	3.03(7)	4.15(6)	4.13(4)	4.20(7)

Water sites with interatomic separations less than 2.5 Å are not likely to be simultaneously occupied. Although data quality did not permit unambiguous distinctions between water and methanol in the pores, it is plausible that both molecules may be found at w3 and w6 sites but are more mobile than the fixed crystallographic positions account for.

Table 15: Bond angles (°) for K-L with m.e. at the investigated pressure points

Pressure (GPa)	P_{amb}	0.29(2)	1.13(2)	1.93(2)
T1- O1 - T1	130.48(28)	124.5(8)	126.5(12)	122.3(11)
T1- O2 - T1	146.841(1)	148.463	152.0(8)	162.1(8)
T2 - O3 - T2	137.01(10)	144.2(4)	140.5(10)	138.5(10)
T2 - O4 - T1	144.07(12)	145.7(4)	147.4(7)	143.8(6
T2 - O5 - T2	141.45(14)	137.6(5)	138.9(10)	140.2(9)
T2 - O6 - T2	153.40(16)	147.6(6)	153.2(11)	154.1(10)
Average	142.2	141.3	143.1	143.5

Table 16: 12-ring channel distances and ellipticity (Å) for K-L with m.e. at the investigated pressure points

Pressure (GPa)	P_{amb}	0.29(2)	1.13(2)	1.93(2)
O1-O1 [001]	9.92(2)	9.98(3)	9.88(3)	9.89(3)
O2-O2 [001]	10.488	10.595	10.43(2)	10.6
O1-O1 [100]	7.5277(4)	7.511(1)	7.458(1)	7.398(1)
12 ring ϵ	1.06	1.06	1.06	1.07

Table 17: 8-ring channel distances and ellipticity (Å) for K-L with m.e. at the investigated pressure points

Pressure (GPa)	P_{amb}	0.29(2)	1.13(2)	1.93(2)
O1-O1 [001]	8.58(2)	8.38(3)	8.44(3)	8.39(3)
O5-O5 [001]	4.68	4.558	4.5	5.104
O5-O5 [100]	3.38(1)	3.41(2)	3.42(2)	3.11(2)
8 ring ϵ	1.83	1.84	1.88	1.72

Table 18: 6-ring channel distances (Å) for K-L with m.e. at the investigated pressure points

Pressure (GPa)	P_{amb}	0.29(2)	1.13(2)	1.93(2)
O3-O5 [001]	5.1860(5)	5.239(2)	5.2578(3)	4.729(2)

GASP simulations

Non-penetrating media

Table 19: Refinement parameters showing how well the simulated K-L models fit the data before refining atomic co-ordinates

Pressure (GPa)	0.19(1)	0.45(1)	0.91(1)	1.31(1)	1.71(2)	2.74(3)	4.15(4)
d-spacing range (Å)	0.6-4	0.6-4	0.4-4	0.48-4	0.4-4	0.6-0.4	0.6-0.4
no. of obs	3140	3881	3634	3512	3809	3089	3183
no. of var	11	22	21	20	25	20	16
a (Å)	18.390(5)	18.349(5)	18.287(7)	18.246(5)	18.178(7)	17.910(15)	17.627(18)
c (Å) 7.4937(2)	7.4796(13)	7.4549(11)	7.4289(16)	7.3980(13)	7.3655(18)	7.257(4)	7.100(5)
volume (Å^3)	2190.6(7)	2173.6(6)	2151.4(9)	2132.8(7)	2107.8(10)	2016.0(21)	1910.6(24)
R_{exp}	6.41	3.77	1.74	3.16	3.21	3.03	2.74
R_{wp}	7.76	5.24	6.04	7.17	6.74	7.43	9.14
reduced χ^2	1.46	1.93	12.04	5.15	4.41	6.00	11.16
GOF	1.21	1.39	3.47	2.27	2.1	2.45	3.34
Average T-O fixed (Å)	1.642	1.642	1.642	1.642	1.642	1.61	1.60

Table 20: Bond angles (°) of simulated K-L structures

Pressure (GPa)	0.19(1)	0.45(1)	0.91(1)	1.31(1)	1.71(2)	2.74(3)	4.15(4)
T1- O1 - T1	125.978	121.6	118.914	116.823	114.379	118.079	112.17
T1- O2 - T1	152.923	157.303	159.992	162.084	164.529	160.826	166.742
T2 - O3 - T2	141.521	142.708	143.305	143.722	144.162	143.278	148.704
T2 - O4 - T1	142.264	139.719	138.009	136.536	134.914	136.781	119.85
T2 - O5 - T2	140.739	141.704	141.791	141.491	141.229	140.089	136.852
T2 - O6 - T2	161.261	162.861	164.223	165.588	166.948	166.401	166.14
Average	144.11	144.32	144.37	144.37	144.36	144.24	141.74

Table 21: 12-ring channel distances and ellipticity (Å) of simulated K-L structures

Pressure (Gpa)	0.19(1)	0.45(1)	0.91(1)	1.31(1)	1.71(2)	2.74(3)	4.15(4)
O1-O1 [001]	9.855	9.798	9.693	9.608	9.504	9.471	9.167
O2-O2 [001]	10.633	10.659	10.683	10.697	10.709	10.48	10.443
O1-O1 [100]	7.479	7.456	7.428	7.397	7.365	7.231	7.117
12 ring ϵ	1.079	1.088	1.102	1.113	1.127	1.107	1.139

Table 22: 8-ring channel distances and ellipticity (Å) of simulated K-L structures

Pressure (Gpa)	0.19(1)	0.45(1)	0.91(1)	1.31(1)	1.71(2)	2.74(3)	4.15(4)
O1-O1 [001]	8.506	8.551	8.601	8.639	8.68	8.455	8.49
O5-O5 [001]	4.734	4.733	4.729	4.724	4.715	4.638	4.611
O5-O5 [100]	3.28	3.243	3.196	3.14	3.085	3.028	2.804
8 ring ϵ	1.797	1.807	1.819	1.829	1.841	1.823	1.841

Table 23: 6-ring channel distances (Å) of simulated K-L structures

Pressure (Gpa)	0.19(1)	0.45(1)	0.91(1)	1.31(1)	1.71(2)	2.74(3)	4.15(4)
O3-O5 [001]	5.241	5.255	5.27	5.28	5.291	5.17	5.159

Table 24: Polyhedral rotation output from GASP: magnitude of T1 anti-rotations in 12 MR at investigated pressures w.r.t P_{amb}

Rx	Ry	Rz	Rotation (°)
		0.19(1) GPa	
0.00	0.00	0.10	5.69
0.00	0.00	-0.10	5.69
		0.46(1) GPa	
0.00	0.00	0.11	6.49
0.00	0.00	-0.11	6.48
		0.91(1) GPa	
0.00	0.00	0.13	7.67
0.00	0.00	-0.13	7.66
		1.31(1) GPa	
0.00	0.00	0.13	7.67
0.00	0.00	-0.13	7.66
		1.71(2) GPa	
0.00	0.00	0.17	9.75
0.00	0.00	-0.17	9.74

Table 25: Polyhedral rotation output from GASP: magnitude of T2 anti-rotations at investigated pressures w.r.t P_{amb}

Rx	Ry	Rz	Rotation (°)
		0.19(1) GPa	
0.04	-0.05	-0.06	5.02
-0.04	0.05	-0.06	5.02
0.04	0.05	0.06	5.02
-0.04	-0.05	0.06	5.02
-0.02	0.06	0.06	5.02
0.02	0.06	-0.06	5.02
-0.02	-0.06	-0.06	5.02
0.02	-0.06	0.06	5.02
-0.07	-0.01	-0.06	5.02
0.07	0.01	-0.06	5.02
-0.07	0.01	0.06	5.02
0.07	-0.01	0.06	5.02
		0.46(1) GPa	
0.05	-0.06	-0.07	5.78
-0.05	0.06	-0.07	5.78
0.05	0.06	0.07	5.77
-0.05	-0.06	0.07	5.77
0.03	0.07	-0.07	5.78
-0.03	-0.07	-0.07	5.78
0.03	-0.07	0.07	5.77
-0.03	0.07	0.07	5.77
-0.08	-0.01	-0.07	5.78
0.08	0.01	-0.07	5.78
-0.08	0.01	0.07	5.77
-0.08	0.01	0.07	5.77

Rx	Ry	Rz	Rotation (°)
		1.31(1) GPa	
0.05	-0.07	-0.08	6.68
-0.05	0.07	-0.08	6.68
0.05	0.07	0.08	6.68
-0.05	-0.07	0.08	6.68
0.03	0.08	-0.08	6.68
-0.03	-0.08	-0.08	6.68
0.03	-0.08	0.08	6.68
-0.03	0.08	0.08	6.68
-0.09	-0.01	-0.08	6.68
0.09	0.01	-0.08	6.68
-0.09	0.01	0.08	6.68
0.09	-0.01	0.08	6.68
		1.71(2) GPa	
0.07	-0.09	-0.10	8.60
-0.07	0.09	-0.10	8.60
0.07	0.09	0.10	8.60
-0.07	-0.09	0.10	8.60
0.04	0.10	-0.10	8.60
-0.04	-0.10	-0.10	8.60
0.04	-0.10	0.10	8.60
-0.04	0.10	0.10	8.60
-0.11	-0.02	-0.10	8.60
0.11	0.02	-0.10	8.60
-0.11	0.02	0.10	8.60
0.11	-0.02	0.10	8.60

Penetrating media

Table 26: Refinement parameters showing how well the simulated K-L models fit the data before refining atomic co-ordinates. At pressures of 0.58 and 3.32 GPa, data quality prevented unambiguous refinements and only lattice parameters could be extracted by the Le Bail method

Pressure (GPa)	0.29(2)	0.58(2)	1.13(2)	1.93(2)	2.89(2)	3.32(4)
d-spacing range (Å)	0.4-4	0.4-4	0.4-4	0.4-4	0.4-4	0.4-4
no. of obs	3881	3881	3881	3881	3881	3881
no. of var	23		20	23	33	
a (Å)	18.362(4)	18.355(6)	18.323(4)	18.295(5)	18.271(9)	18.255(1)
c (Å)	7.5094(11)	7.497(2)	7.4590(13)	7.3950(13)	7.3361(25)	7.314(2)
volume ($Å_3$)	2192.6(6)	2187.6(9)	2168.6(6)	2143.6(7)	2121.0(12)	2110(2)
R_{exp}	3.85		3.93	3.10	4.21	
$R_{wp} =$	4.58		4.28	4.96	5.31	
reduced $\chi^2 = (R_{wp}/R_{exp})^2$	1.42		1.19	2.56	1.59	
$GOF = (R_{wp}/R_{exp})$	1.19		1.09	1.6	1.26	
Average T-O fixed (Å)	1.642	1.642	1.642	1.642	1.642	1.642

Table 27: Bond angles (°) of simulated K-L structures

Pressure (GPa)	0.29(2)	0.58(2)	1.13(2)	1.93(2)	2.89(3)	3.32(4)
T1- O1 - T1	122.974	122.333	120.523	118.902	117.249	116.718
T1- O2 - T1	155.929	156.569	158.382	160.003	161.657	162.189
T2 - O3 - T2	142.484	142.63	142.999	143.236	143.488	143.525
T2 - O4 - T1	141.263	140.768	139.287	137.492	135.804	135.176
T2 - O5 - T2	142.969	142.868	142.307	140.713	135.804	138.675
T2 - O6 - T2	160.529	161.055	162.778	165.424	167.64	168.516
Average	144.36	144.37	144.38	144.30	143.61	144.13

Table 28: 12-ring channel distances and ellipticity (Å) of simulated K-L structures

Pressure (GPa)	0.29(2)	0.58(2)	1.13(2)	1.93(2)	2.89(3)	3.32(4)
O1-O1 [001]	9.849	9.825	9.756	9.693	9.626	9.604
O2-O2 [001]	10.644	10.651	10.669	10.683	10.694	10.698
O1-O1 [100]	7.508	7.497	7.46	7.397	7.339	7.314
12 ring ϵ	1.081	1.084	1.094	1.102	1.111	1.114

Table 29: 8-ring channel distances and ellipticity (Å) of simulated K-L structures

Pressure (GPa)	0.29(2)	0.58(2)	1.13(2)	1.93(2)	2.89(3)	3.32(4)
O1-O1 [001]	8.516	8.53	8.569	8.606	8.64	8.651
O5-O5 [001]	4.73	4.73	4.731	4.732	4.73	4.729
O5-O5 [100]	3.349	3.328	3.257	3.131	3.02	2.973
8 ring ϵ	1.800	1.803	1.811	1.819	1.827	1.829

Table 30: *D6r* distances (Å) of simulated K-L structures

Pressure (GPa)	0.29(2)	0.58(2)	1.13(2)	1.93(2)	2.89(3)	3.32(4)
O3-O5 [001]	5.249	5.252	5.262	5.269	5.275	5.277

Table 31: Polyhedral rotation output from GASP: magnitude of initial T1 anti-rotations in the 12MR at investigated pressures w.r.t P_{amb}

Rx	Ry	Rz	Rotation (°)
		0.29(2) GPa	
0.00	0.00	0.11	6.20
0.00	0.00	-0.11	6.19

Table 32: Polyhedral rotation output from GASP: magnitude of initial T2 anti-rotations at investigated pressures w.r.t P_{amb}

Rx	Ry	Rz	Rotation (°)
		0.29(2) GPa	
0.03	-0.05	-0.06	4.76
-0.03	0.05	-0.06	4.76
0.03	0.05	0.06	4.76
-0.03	-0.05	0.06	4.76
0.03	0.05	-0.06	4.76
-0.03	-0.05	-0.06	4.76
0.03	-0.05	0.06	4.76
-0.03	0.05	0.06	4.76
-0.05	0.00	-0.06	4.76
0.05	0.00	-0.06	4.76
-0.05	0.00	0.06	4.76
0.05	0.00	0.06	4.76

Table 33: Polyhedral rotation output from GASP: magnitude of T1 anti-rotations in 12 MR at investigated pressures w.r.t filled structure at 0.29(2) GPa

Rx	Ry	Rz	Rotation (°)
		1.13(2) GPa	
0.00	0.00	0.02	0.92
0.00	0.00	-0.02	0.92
		1.93(2) GPa	
0.00	0.00	0.03	1.57
0.00	0.00	-0.03	1.57
		2.89(2) GPa	
0.00	0.00	0.04	2.27
0.00	0.00	-0.04	2.27
		3.32(4) GPa	
0.00	0.00	0.04	2.50
0.00	0.00	-0.04	2.50

Table 34: Polyhedral rotation output from GASP: magnitude of T2 anti-rotations at investigated pressures w.r.t filled structure at 0.29(2) GPa

Rx	Ry	Rz	Rotation (°)
		1.13(2) GPa	
0.01	-0.02	-0.01	1.34
-0.01	0.02	-0.01	1.34
0.01	0.02	0.01	1.34
-0.01	-0.02	0.01	1.34
0.01	0.02	-0.01	1.34
-0.01	-0.02	-0.01	1.34
0.01	-0.02	0.01	1.34
-0.01	0.02	0.01	1.34
-0.02	0.00	-0.01	1.34
0.02	0.00	-0.01	1.34
-0.02	0.00	0.01	1.34
0.02	0.00	0.01	1.34
		1.93(2) GPa	
0.03	-0.03	-0.01	2.76
-0.03	0.03	-0.01	2.76
0.03	0.03	0.01	2.76
-0.03	-0.03	0.01	2.76
0.01	0.04	-0.01	2.76
-0.01	-0.04	-0.01	2.76
0.01	-0.04	0.01	2.76
-0.01	0.04	0.01	2.76
-0.04	-0.01	-0.01	2.76
0.04	0.01	-0.01	2.76
-0.04	0.01	0.01	2.76
0.04	-0.01	0.01	2.76

	2.89(3) GPa		
0.05	-0.05	-0.02	4.07
-0.05	0.05	-0.02	4.07
0.05	0.05	0.02	4.07
-0.05	-0.05	0.02	4.07
0.02	0.06	-0.02	4.07
-0.02	-0.06	-0.02	4.07
0.02	-0.06	0.02	4.07
-0.02	0.06	0.02	4.07
-0.07	-0.01	-0.02	4.07
0.07	0.01	-0.02	4.07
-0.07	0.01	0.02	4.07
0.07	-0.01	0.02	4.07
	3.32(4) GPa		
0.05	-0.06	-0.02	4.57
-0.05	0.06	-0.02	4.57
0.05	0.06	0.02	4.57
-0.05	-0.06	0.02	4.57
0.02	0.07	-0.02	4.57
-0.02	-0.07	-0.02	4.57
0.02	-0.07	0.02	4.57
-0.02	0.07	0.02	4.57
-0.07	-0.02	-0.02	4.57
0.07	0.02	-0.02	4.57
-0.07	0.02	0.02	4.57
0.07	-0.02	0.02	4.57

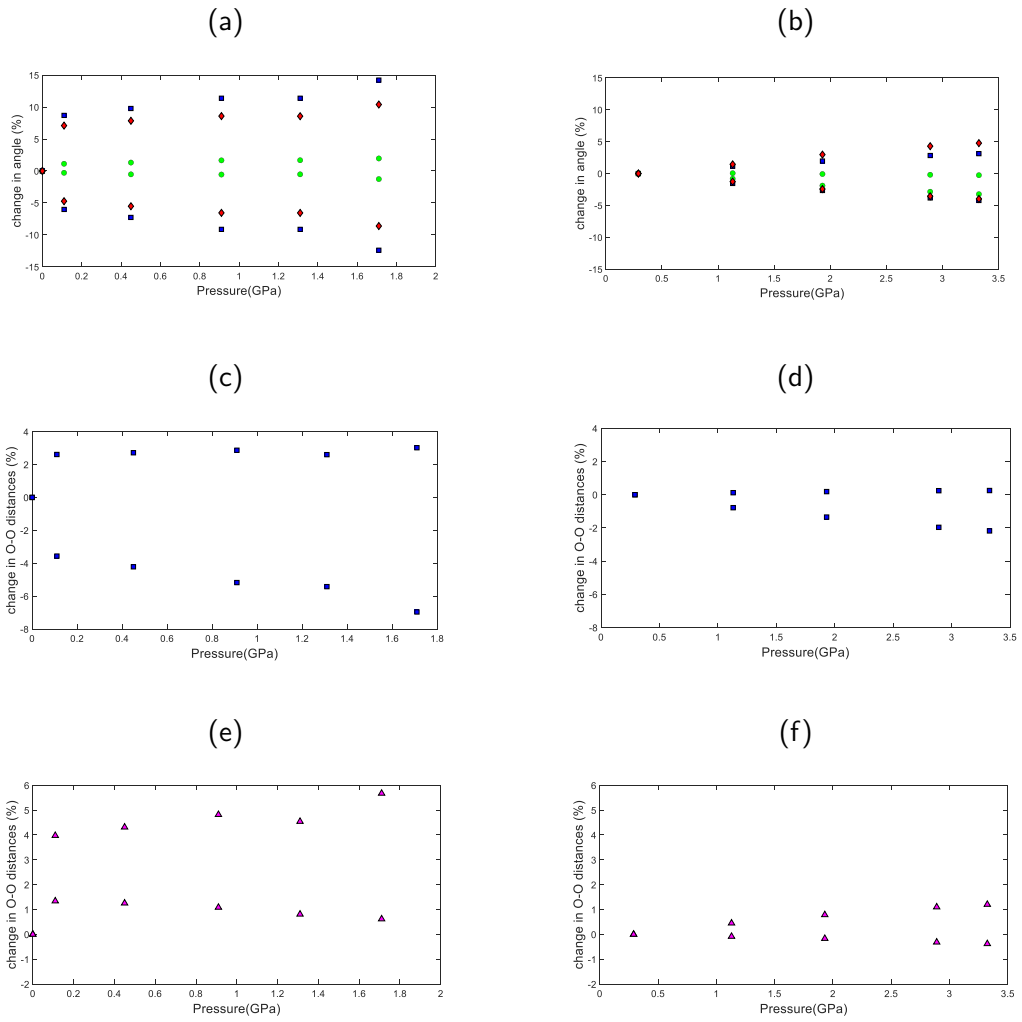

Figure 4: Structural evolution of T-O-T bond angles and O-O channel distances with pressure. (a) and (b) show cooperative increase and decrease in bond angles for empty and filled K-LTL, respectively. 12-ring angles in *a*-plane are shown in blue squares (T1-O1-T1 decrease and T1-O2-T2 increase), *d6r* angles in *a*-plane are shown in green circles (T2-O3-T2 increase and T2-O5-T2 decrease) and angles in *c*-plane are shown in red diamonds (T2-O6-T2 increase and T2-O4-T1 decrease). (c-f) show changes in the largest and shortest O-O distances with pressure for 12-ring channel in non-penetrating PTM, 12-ring channel in penetrating media, 8-ring channel in non-penetrating media and 8-ring channel in penetrating media, respectively.

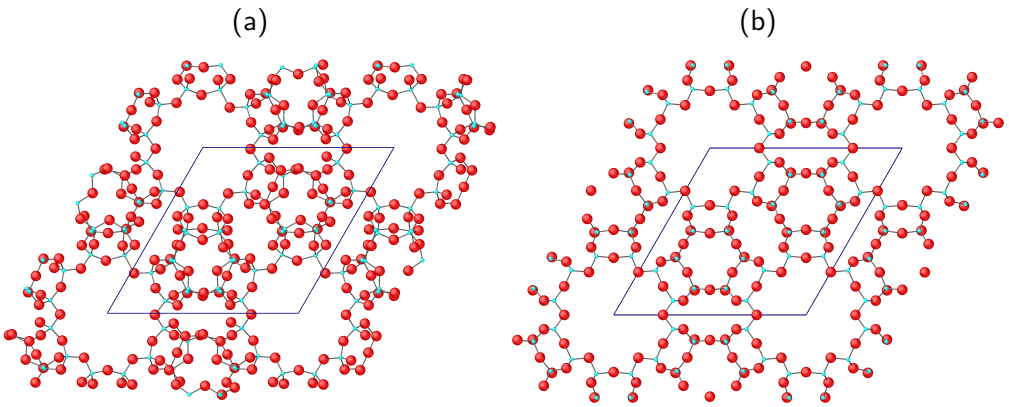

Figure 5: GASP-simulated structures of the empty K-LTL framework outside the flexibility window at 4.15(4) GPa, using T-O bond lengths of (a) 1.642 Å, leading to steric clashes of oxygen atoms and (b) bond lengths of 1.60 Å, where geometric relaxation can be achieved.

GASP Input files

Example flexibility window-search script using GASP's "search" function. This was used to find the grey window limits for the hexagonal LTL unit cell, as shown in Figure 6 of the MS.

```
    ELEMENT
si 0.26
o 1.35
k 1.33
/ELEMENT
POLY
tet si o 1.642
/POLY
OPTION
relax
smallmove 1e-6
smallmis 1e-3
search hex
/OPTION
INPUT
structure LTL_P1.cif
bonding LTL_P1.bonding
```

/INPUT
OUTPUT
window LTL-window-1
/OUTPUT

Example of a single-point GASP input file used to relax the structure at a specific point. This was used to find relaxed, high-pressure structures within the flexibility window, plotted in Figure 6 of the MS. The "new cell" parameters are specified using those extracted from LeBail fitting of data at each pressure point.

ELEMENT
si 0.26
o 1.35
k 1.33
/ELEMENT
POLY
tet si o 1.642
/POLY
OPTION
relax
smallmove 1e-6
smallmis 1e-3
/OPTION
INPUT
structure LTL_P1.cif
bonding LTL_P1.bonding
new cell 18.39 18.39 7.48 90 90 120
/INPUT
OUTPUT
structure LTL_0.19GPa.cif
/OUTPUT